Vapor–liquid equilibria of carbon dioxide with isopropyl acetate, diethyl carbonate and ethyl butyrate at elevated pressures

Chen-His Cheng, Yan-Ping Chen *

Department of Chemical Engineering, National Taiwan University, Taipei 106, Taiwan, ROC

Abstract

Vapor–liquid equilibria for carbon dioxide with three esters of isopropyl acetate, diethyl carbonate and ethyl butyrate were measured in this study at 308.45, 313.45 and 318.55 K and at elevated pressures up to 8.9 MPa. A static type phase equilibrium apparatus with visual sapphire windows was used in the experimental measurements. Equilibrium compositions in both vapor and liquid phases and the vapor–liquid equilibrium (VLE) constants are reported. The solubility for each ester compound in the vapor phase is in the order of 10^{-3} mole fraction. These new VLE data were correlated using either the equation of state (EOS) or activity coefficient model. It is shown that the Peng–Robinson or Soave–Redlich–Kwong EOS with van der Waals mixing rules gives satisfactory results. These VLE data are also well correlated by the UNIQUAC activity coefficient model with two optimally fitted binary interaction parameters.
© 2005 Elsevier B.V. All rights reserved.

Keywords: Vapor–liquid equilibrium; High pressure; Binary mixtures

1. Introduction

Vapor–liquid equilibrium (VLE) data at high pressures are important for chemical process such as supercritical extraction. Carbon dioxide is the most commonly used supercritical fluid. Although many phase equilibrium data have been presented in literature [1–3], VLE or gas solubility for carbon dioxide with ester compounds is still inadequate. In our previous studies [4–6], we have measured the VLE data for carbon dioxide with several ester compounds using a semi-flow apparatus up to 13 MPa. In this study, we measured the VLE data for three binary mixtures for carbon dioxide with isopropyl acetate, diethyl carbonate and ethyl butyrate using a static apparatus with visual sapphire windows. Isopropyl acetate and ethyl butyrate are used as perfume or aroma additives for cosmetics and food industries. Diethyl carbonate is used in organic synthesis or the production of resin. The experimental temperatures are at 308.45, 313.45 and 318.55 K, with pressure range from 3 to 8.9 MPa. To our knowledge, the

VLE data for these systems at the above conditions are not available in literature. This study presents new phase equilibrium data at elevated pressures. The measured data were also correlated using either the equation of state (EOS) with empirical mixing rules, or the commonly used activity coefficient model.

2. Experimental

2.1. Chemicals

Liquefied carbon dioxide at high pressure with purity greater than 99.9 mass% was purchased from San-Fu Chemical Co. (Taiwan). Isopropyl acetate, diethyl carbonate and ethyl butyrate were purchased from Acros. The properties for pure ester compounds were measured in this study and the results are shown in Table 1. The refractive indices were measured at 293.15 K using an Abbe refractometer, Atago 3T, with an accuracy of ±0.0001. The densities of pure compounds were measured at 293.15 or 298.15 K using the Anton Paar DMA 58 density meter with an accuracy of

* Corresponding author. Fax: +886 2 2362 3040.
  E-mail address: ypchen@ntu.edu.tw (Y.-P. Chen).

Table 1
Comparison of the measured refractive indices and densities of pure solvents with literature data

Component	Refractive index (293.15 K)		Density (kg m^{-3})		GC purity (mass%)
	Experiment	Literature [18]	Experiment	Literature	
Ethanol	1.3592	1.3594	789.4[a]	789.4 [17]	>99.9
Isopropyl acetate	1.3751	1.3750	866.4[b]	870.2 [19]	>99.5
Diethyl carbonate	1.3830	1.3829	969.2[b]	969.3 [19]	>99.6
Ethyl butyrate	1.3899	1.3900	879.0[a]	878.9 [17]	>99.3

　[a] $T = 293.15$ K.
　[b] $T = 298.15$ K.

± 0.1 kg m^{-3}. The measured refractive index and densities agree well with literature data. The purities of all chemicals are greater than 99 mass% that were measured using gas chromatograph (GC). These chemicals were used without further purification.

2.2. Apparatus

The phase equilibrium apparatus of this study is shown in Fig. 1. It is a static type apparatus with circulation of the liquid phase. There are mainly three sections for the input of sample, the high-pressure equilibrium cell and the analysis for compositions of the equilibrium phases. The equilibrium cell was made by stainless steel with an internal volume of 320 mL. There are six visual sapphire windows (Sitec, Switzerland) in the equilibrium cell for the visual observation of the phase behavior. The pressure in the equilibrium cell was measured by a Druck pressure gauge (PDCR-4031) with a digital indicator (DPI-281). The range of the pressure gauge is up to 700 bar, with a resolution of ± 0.35 bar and an estimated accuracy of $\pm 0.05\%$ of the digital reading value. The temperature in the equilibrium cell was measured by a K-type thermocouple. The digital indicator has a resolution of 0.01 K and an estimated accuracy of ± 0.1 K. The liquid phase was recir-

culated to reach the equilibrium condition using a duplex metering pump (LCD, Analytical Inc.). Equilibrium samples were taken by the sampling valves. The vapor sampling valve (Valco, 6UW) has an external loop with volume of 20 μL. The liquid sampling valve (Rheodyne, 7010) has an external loop with volume of 5 μL. On-line analyses for the equilibrium compositions have been carried out using GC (Shimadzu 14B). The GC was equipped with a thermal conductivity detector (TCD) and a column 2 m in length with 1/8 in. diameter packed with Porapak P. The equilibrium cell and the sampling valves were all immersed in a water bath controlled by a PID controller. The estimated accuracy for measured temperature is ± 0.1 K. Heating tapes were used for lines between the bath and GC to keep the temperature at ± 0.1 K of a desired value through a PID controller. Helium was used as the carrier gas with a flow rate of 45 mL min^{-1}. The TCD detector was kept at 483.15 K. The column of the GC was kept at 373.15 K for CO_2 + isopropyl acetate, and at 413.15 K for the other two systems. The current of TCD was 70 mA.

2.3. Calibration procedures

The volumes of the sampling loops were calibrated using the similar procedures in literature [7,8]. These loops were
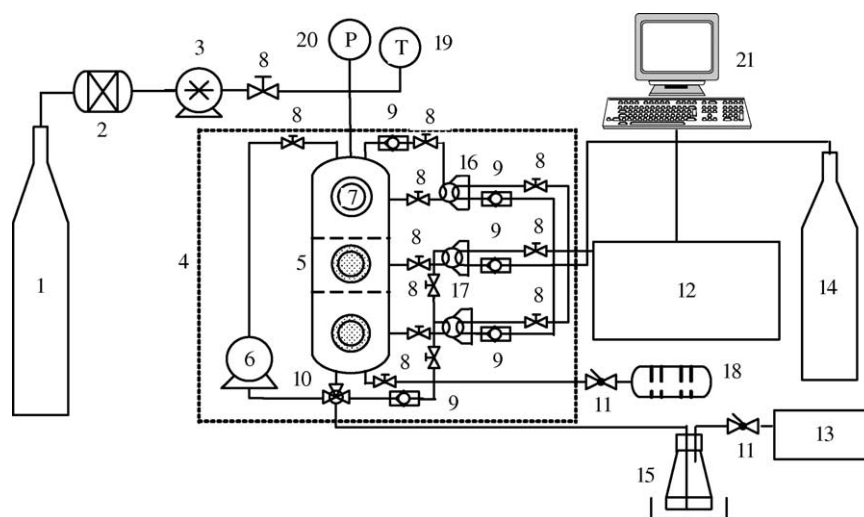

Fig. 1. Schematic diagram of the high-pressure experimental apparatus used in this study. (1) CO_2 cylinder, (2) cooler, (3) liquid pump, (4) water bath, (5) high-pressure vessel, (6) circulation pump, (7) sapphire window unit, (8) needle valve, (9) check valve, (10) two-way valve, (11) ball valve, (12) GC, (13) vacuum pump, (14) He cylinder, (15) degas/feeding unit, (16) gas sampling valve, (17) liquid sampling valve, (18) drain bottle, (19) thermocouple, (20) pressure transmitter and (21) analysis unit.

calibrated using distilled water controlled at 298.15 K. With the measured weights of the sampling loops and the known density of water at the given temperature, the loop volumes were determined as 21.83 and 4.52 μL for the vapor and liquid sampling loops, respectively.

The on-line GC method was used to analyze the equilibrium compositions. The calibration of GC was made by plotting the peak areas against the number of moles of the pure gas or liquid sample, as was presented by previous investigators [9,10]. For the liquid samples, the weighting method on a digital balance (Mettler Toledo AX105, $\pm 2 \times 10^{-5}$ g) was used to evaluate the weight and number of moles. The GC peak areas for three ester compounds were plotted against their number of moles, respectively. The third-order polynomial curve fitting was found satisfactory for these pure liquid sample calibration curves. Calibrations for the gas samples were performed when carbon dioxide was pressurized to a desired value in an isothermal water bath. With the gas sampling valves connected to GC, the peak areas were obtained at various T and P conditions. The molar volumes for carbon dioxide at various T and P conditions were calculated using the data base of NIST [11]. From the molar volumes of carbon dioxide and the loop volumes of the gas sampling valve, numbers of moles of carbon dioxide were determined in the calibrations. Third-order polynomial curves were also observed for gas phase calibration at each isotherm.

2.4. Experimental procedures

The experimental apparatus was evacuated to a sub-atmospheric pressure and the CO_2 + ester compounds were injected through the system for cleaning before each VLE measurement. The liquid ester solvent was degassed for 20 min before charging into the equilibrium cell immersed in a water bath. The CO_2 was then fed into the system through the high-pressure pump to a desired pressure. The liquid phase sample was recirculated through a metering pump at a flow rate of 9 mL min^{-1} in order to enhance rapid equilibrium. At all experimental conditions, equilibrium vapor and liquid phases were visually observed after 12 h of recirculation through the windows of the equilibrium cell. The system was then settled for 3.5 h to reach the final equilibrium. The final pressure reading was recorded and the equilibrium compositions of the two phases were analyzed by GC. During the liquid sampling procedures, the flow rate of the metering pump was carefully controlled to minimize the disturbance of the equilibrium state. The equilibrium compositions were the averaged values of more than five repeated measurements. The sampling loops were then evacuated to remove any residual. The accuracy of the equilibrium compositions was estimated as ± 0.002 mole fraction in this study.

3. Results and discussion

The VLE measurements for the binary mixture of CO_2 + ethanol were first carried out and compared with liter-
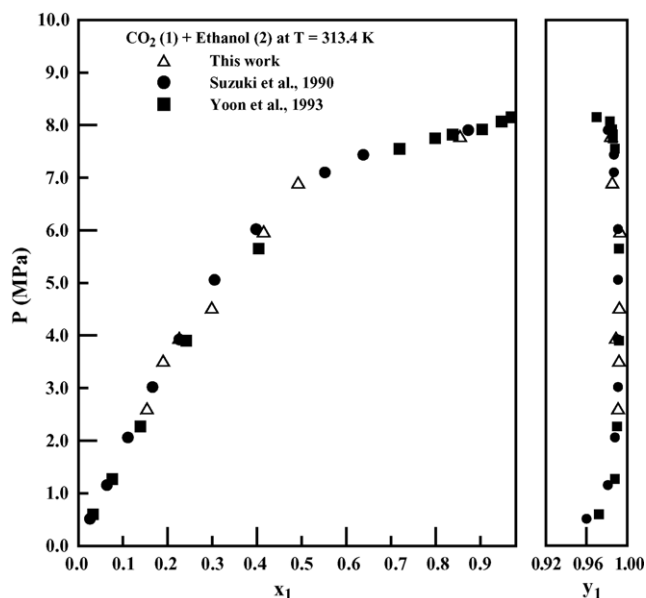

Fig. 2. Comparison of the P–x–y data for the binary mixture of CO_2 (1) + ethanol (2) at 313.4 K.

ature data [7,9]. The result is presented graphically in Fig. 2. The measured data in this study agree well with those in previous literature and the reliability of the apparatus in this study is confirmed. The measured equilibrium compositions and the corresponding K_1 values ($K_1 = y_1/x_1$) at various temperature and pressure states for three binary mixtures are shown in Tables 2–4, respectively. The standard deviations for the equilibrium liquid and vapor compositions from repeated measurements are less than 10^{-3} and 10^{-4} mole fractions, respectively. Graphical representations of the VLE results are shown in Figs. 3–5, respectively. Generally, the solubility of CO_2 in the liquid phase increases with pressure but decreases with temperature. The vapor phase contains mainly CO_2 of more than 99 mol%.
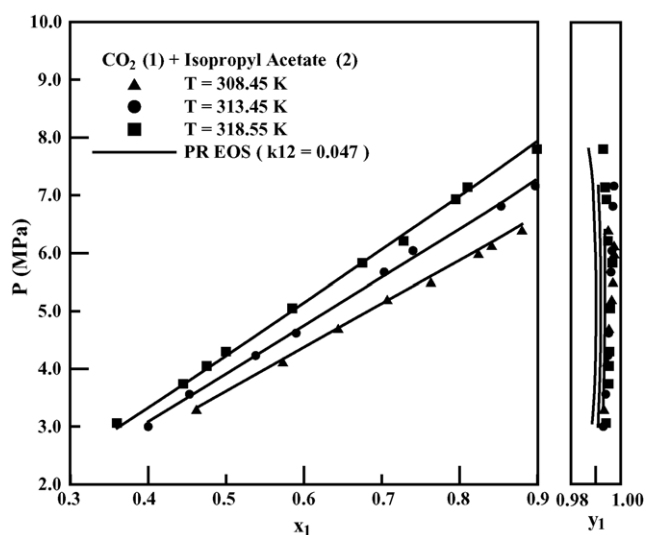

Fig. 3. VLE results of the binary mixture of CO_2 (1) + isopropyl acetate (2).

Table 2
Experimental VLE results for the binary mixture of CO_2 (1) + isopropyl acetate (2)

Pressure (MPa)	Equilibrium composition		Equilibrium constant, K_1
	x_1	y_1	
$T = 308.45$ K			
3.30	0.462	0.9933	2.150
4.12	0.573	0.9946	1.736
4.70	0.644	0.9953	1.545
5.20	0.707	0.9964	1.409
5.50	0.763	0.9969	1.307
5.99	0.824	0.9974	1.210
6.13	0.841	0.9974	1.186
6.40	0.880	0.9950	1.131
$T = 313.45$ K			
3.08	0.400	0.9930	2.483
3.56	0.453	0.9940	2.194
4.23	0.538	0.9949	1.849
4.62	0.590	0.9952	1.687
5.67	0.703	0.9961	1.417
5.94	0.740	0.9965	1.347
6.81	0.853	0.9969	1.169
7.16	0.897	0.9973	1.112
$T = 318.55$ K			
3.06	0.360	0.9941	2.761
3.74	0.445	0.9951	2.236
4.05	0.475	0.9953	2.095
4.30	0.500	0.9955	1.991
5.05	0.585	0.9958	1.702
5.83	0.675	0.9967	1.477
6.21	0.728	0.9949	1.367
6.93	0.795	0.9943	1.251
7.14	0.810	0.9937	1.227
7.80	0.899	0.9929	1.104

Table 3
Experimental VLE results for the binary mixture of CO_2 (1) + diethyl carbonate (2)

Pressure (MPa)	Equilibrium composition		Equilibrium constant, K_1
	x_1	y_1	
$T = 308.45$ K			
4.72	0.500	0.9947	1.989
5.06	0.530	0.9948	1.877
5.50	0.585	0.9950	1.701
5.80	0.625	0.9955	1.593
6.07	0.682	0.9958	1.460
6.50	0.730	0.9968	1.365
6.75	0.800	0.9973	1.247
6.94	0.840	0.9968	1.187
7.14	0.892	0.9961	1.117
$T = 313.45$ K			
4.50	0.450	0.9950	2.211
5.12	0.505	0.9961	1.972
5.46	0.545	0.9969	1.829
6.13	0.610	0.9978	1.636
6.66	0.685	0.9983	1.457
7.08	0.745	0.9977	1.339
7.42	0.781	0.9975	1.277
7.50	0.795	0.9965	1.253
7.69	0.840	0.9960	1.186
$T = 318.55$ K			
4.30	0.400	0.9933	2.483
5.00	0.460	0.9935	2.160
5.21	0.475	0.9947	2.094
5.73	0.523	0.9951	1.903
6.13	0.565	0.9963	1.763
6.85	0.619	0.9975	1.611
7.20	0.660	0.9977	1.512
7.50	0.701	0.9970	1.422
7.80	0.750	0.9960	1.328
8.20	0.780	0.9940	1.274
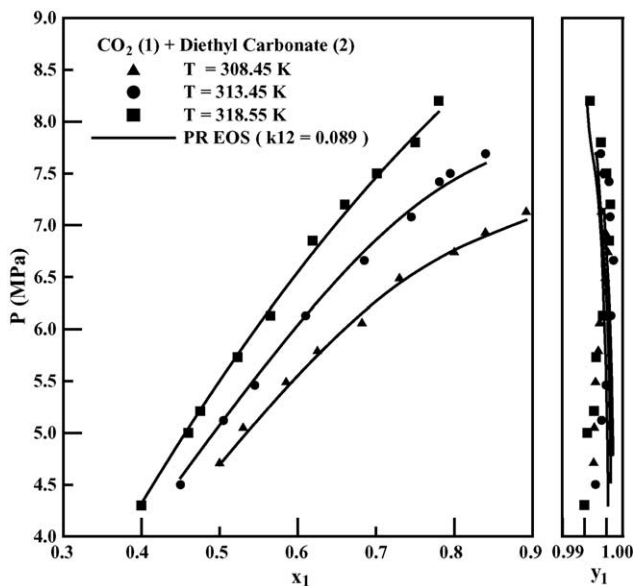
The VLE data measured in this study were correlated by the most commonly used equation of state method. The Peng–Robinson EOS [12]:

$$p = \frac{RT}{v - b} - \frac{a}{v(v + b) + b(v - b)} \tag{1}$$

$$a = 0.45724 \frac{R^2 T_c^2}{P_c} \alpha(T) \tag{2}$$

$$b = 0.07780 \frac{RT_c}{P_c} \tag{3}$$

$$\alpha(T) = \left[1 + (0.37464 + 1.54226\omega - 0.26992\omega^2) \times \left(1 - \sqrt{\frac{T}{T_c}} \right) \right]^2 \tag{4}$$

and the Soave–Redlich–Kwong EOS [13]:

$$P = \frac{RT}{v - b} - \frac{a}{v(v + b)} \tag{5}$$

Fig. 4. VLE results of the binary mixture of CO_2 (1) + diethyl carbonate (2).

Table 4
Experimental VLE results for the binary mixture of CO_2 (1) + ethyl butyrate (2)

Pressure (MPa)	Equilibrium composition		Equilibrium constant, K_1
	x_1	y_1	
$T = 308.45$ K			
4.80	0.480	0.9947	2.072
5.30	0.530	0.9958	1.879
5.65	0.580	0.9966	1.718
6.00	0.630	0.9974	1.583
6.30	0.670	0.9968	1.488
6.60	0.725	0.9953	1.373
6.80	0.810	0.9940	1.227
$T = 313.45$ K			
4.60	0.430	0.9957	2.316
5.10	0.480	0.9961	2.075
5.70	0.535	0.9969	1.863
6.20	0.595	0.9978	1.677
6.70	0.650	0.9983	1.536
7.05	0.690	0.9977	1.446
7.40	0.755	0.9965	1.320
7.90	0.820	0.9950	1.213
$T = 318.55$ K			
4.55	0.395	0.9960	2.522
4.90	0.430	0.9965	2.317
5.40	0.470	0.9969	2.121
6.00	0.530	0.9971	1.881
6.60	0.580	0.9973	1.719
7.20	0.640	0.9985	1.560
8.10	0.760	0.9960	1.311
8.90	0.860	0.9940	1.156
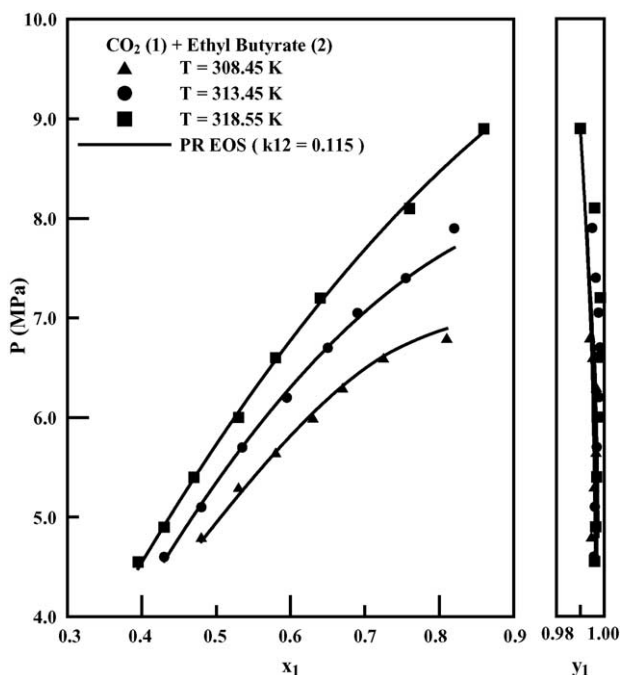
Table 5
Pure component properties used in this work [18]

Component	T_c (K)	P_c (MPa)	v_c (m^3 kmol^{-1})	ω
Carbon dioxide	304.19	7.38	0.094	0.228
Ethanol	516.25	6.38	0.167	0.637
Isopropyl acetate	538.00	3.58	0.336	0.355
Diethyl carbonate	576.00	3.39	0.356	0.485
Ethyl butyrate	566.00	3.06	0.421	0.463

$$a = 0.42748 \frac{R^2 T_c^2}{P_c} \alpha(T) \tag{6}$$

$$b = 0.08664 \frac{R T_c}{P_c} \tag{7}$$

$$\alpha(T) = \left[1 + (0.48 + 1.574\omega - 0.176\omega^2) \left(1 - \sqrt{\frac{T}{T_c}} \right) \right]^2 \tag{8}$$

were employed in these calculations. The EOS parameters were determined from the critical constants of pure fluids that are listed in Table 5. Various mixing rules were used to evaluate the EOS parameters for fluid mixtures. For the traditional van der Waals one-fluid (VDW1) mixing rule, we have:

$$a_m = \sum \sum x_i x_j (a_i a_j)^{0.5} (1 - k_{ij}) \tag{9}$$

$$b_m = \sum x_i b_i \tag{10}$$

where k_{ij} is the binary interaction parameter. If one additional binary interaction parameter is used for b_m, we have the VDW2 mixing rule:

$$b_m = \sum \sum x_i x_j \frac{b_i + b_j}{2} (1 - l_{ij}) \tag{11}$$

The optimally fitted temperature-independent binary interaction parameters were determined through bubble point calculations by minimizing the absolute average deviation (AAD) in calculated equilibrium pressure and compositions.

The other Panagiotoupoulos–Reid (PR) mixing rules [14] give a composition dependent model. In the PR mixing model, the EOS energy parameter is:

$$a_m = \sum \sum x_i x_j (a_i a_j)^{0.5} [1 - k_{ij} + (k_{ij} - k_{ji}) x_i] \tag{12}$$

and the volume parameter is given by Eq. (11). Although the PR mixing model has limit for the extension to multicomponent mixtures, it is applicable in correlating binary VLE data.

Besides the van der Waals type mixing models, a group-contribution mixing model proposed by Huron and Vidal [15] was also used in this study. Applying this model, the excess Gibbs energy calculated from an EOS at an infinite pressure reference state was set equal to that calculated from the UNI-QUAC [16] activity coefficient model. Two binary parameters of the UNIQUAC model were determined by regressing the

Fig. 5. VLE results of the binary mixture of CO_2 (1) + ethyl butyrate (2).

Table 6
Correlated results of experimental VLE data of three binary mixtures using various EOS and mixing rules

Mixing rule	Peng–Robinson EOS					Soave–Redlich–Kwong EOS				
	k_{12}	l_{12} (or k_{21})	AADP (%)	$10^2 \Delta y_1$	AADK$_1$ (%)	k_{12}	l_{12} (or k_{21})	AADP (%)	$10^2 \Delta y_1$	AADK$_1$ (%)
CO_2 (1) + isopropyl acetate (2)										
VDW1	0.047		1.15	0.41	0.71	0.048		1.25	0.34	0.77
VDW2	0.043	−0.010	1.07	0.43	0.69	0.043	−0.012	1.13	0.37	0.71
Panagiotopoulos–Reid	0.060	0.047	1.07	0.43	0.68	0.064	0.475	1.14	0.36	0.74
CO_2 (1) + diethyl carbonate (2)										
VDW1	0.089		0.91	0.17	0.50	0.091		0.84	0.17	0.50
VDW2	0.093	0.007	0.79	0.17	0.49	0.094	0.005	0.78	0.17	0.50
Panagiotopoulos–Reid	0.078	0.090	0.79	0.18	0.45	0.083	0.092	0.78	0.17	0.44
CO_2 (1) + ethyl butyrate (2)										
VDW1	0.115		0.65	0.75	0.41	0.121		0.68	0.73	0.45
VDW2	0.114	−0.003	0.62	0.75	0.57	0.119	−0.003	0.66	0.73	0.44
Panagiotopoulos–Reid	0.119	0.114	0.62	0.75	0.42	0.126	0.120	0.66	0.73	0.51

AADP (%) $= \frac{100}{n} \sum_{k=1}^{n} \frac{|P^{\exp} - P^{\rm cal}|_k}{P_k^{\exp}}$, $\Delta y_1 = \frac{1}{n} \sum_{k=1}^{n} |y_1^{\rm cal} - y_1^{\exp}|_k$ and AADK$_1$ (%) $= \frac{100}{n} \sum_{k=1}^{n} \left| \frac{K_1^{\rm cal} - K_1^{\exp}}{K_1^{\exp}} \right|_k$. The summation is over all data points k.

experimental VLE data through the minimization of the following objective function:

$$\mathrm{obj} = \sum \left| \frac{P^{\exp} - P^{\rm cal}}{P^{\exp}} \right| + \sum |y_1^{\exp} - y_1^{\rm cal}| \qquad (13)$$

The optimally fitted binary interaction parameters from either the PR or SRK EOS using various mixing rules are listed in Table 6. These binary interaction parameters were empirically obtained and no relationship with respect to the physical properties of solutes was attempted. It is shown that the experimental VLE data and K_1 values are satisfactorily correlated by either EOS and mixing rules with optimal binary interaction parameters. The VDW1 mixing rules are the simplest with only one temperature-independent binary interaction parameter. The calculated results with the VDW1 mixing rules are also shown in Figs. 3–5. Table 7 shows the best-fitted binary parameters of the UNIQUAC model and the correlation results for three binary systems. It is again demonstrated that satisfactory calcula-

tion results for bubble point pressure and composition are obtained.

4. Conclusion

VLE measurements for carbon dioxide with isopropyl acetate, diethyl carbonate and ethyl butyrate are presented at 308.45, 313.45 and 318.55 K and pressure up to 8.9 MPa. The VLE data are correlated using the cubic type Peng–Robinson or Soave–Redlich–Kwong equations of state with various mixing rules. The optimally fitted binary parameters are reported and the correlation results are satisfactorily observed.

List of symbols
a, b	equation of state parameters
k, l	binary interaction parameters
P	pressure
R	gas constant
T	temperature
v	molar volume
x	mole fraction in the liquid phase
y	mole fraction in the vapor phase

Greek letter
ω	acentric factor

Subscripts
c	critical property
i, j	component i or j
m	mixture property

Table 7
Correlated results of the experimental VLE data of three binary mixtures by the Huron–Vidal mixing rule with the UNIQUAC activity coefficient model

EOS	A_{12} (kJ mol^{-1})	A_{21} (kJ mol^{-1})	AADP (%)	$10^2 \Delta y_1$
CO_2 (1) + isopropyl acetate (2)				
PR	0.581	1.148	1.010	0.423
SRK	0.406	1.262	1.068	0.358
CO_2 (1) + diethyl carbonate (2)				
PR	1.858	0.636	0.837	0.175
SRK	1.743	0.641	0.820	0.171
CO_2 (1) + ethyl butyrate (2)				
PR	1.887	1.273	0.751	0.749
SRK	1.809	1.250	0.702	0.728

AADP (%) $= \frac{100}{n} \sum_{k=1}^{n} \frac{|P^{\exp} - P^{\rm cal}|_k}{P_k^{\exp}}$ and $\Delta y_1 = \frac{1}{n} \sum_{k=1}^{n} |y_1^{\rm cal} - y_1^{\exp}|_k$. The summation is over all data points k. Parameter $A_{ij} = u_{ij} - u_{jj}$, where u_{ij} is the energy of interaction between molecules i and j. The UNIQUAC equations were taken from Ref. [16].

Acknowledgement

References

[1] R.E. Fornari, P. Alessi, I. Kikic, Fluid Phase Equilib. 57 (1990) 1–33.

[2] R. Dohrn, G. Brunner, Fluid Phase Equilib. 106 (1995) 213–282.

[3] M. Christov, R. Dohrn, Fluid Phase Equilib. 202 (2002) 153–218.

[4] K.W. Cheng, S.J. Kuo, M. Tang, Y.P. Chen, J. Supercrit. Fluids 18 (2000) 87–99.

[5] K.W. Cheng, M. Tang, Y.P. Chen, Fluid Phase Equilib. 181 (2001) 1–16.

[6] L.C. Feng, K.W. Cheng, M. Tang, Y.P. Chen, J. Supercrit. Fluids 21 (2001) 111–121.

[7] J.H. Yoon, H.S. Lee, H. Lee, J. Chem. Eng. Data 38 (1993) 53–55.

[8] T. Laursen, P. Rasmussen, S.I. Andersen, J. Chem. Eng. Data 47 (2002) 198–202.

[9] K. Suzuki, H. Sue, M. Itou, R.L. Smith, H. Inomata, K. Arai, S. Sato, J. Chem. Eng. Data 35 (1990) 63–66.

[10] J.H. Yoon, H.S. Lee, B.H. Chung, Fluid Phase Equilib. 102 (1994) 287–292.

[11] http://webbook.nist.gov/chemistry.

[12] D.Y. Peng, D.B. Robinson, Ind. Eng. Chem. Fundam. 15 (1976) 59–64.

[13] G. Soave, Chem. Eng. Sci. 27 (1972) 1197–1203.

[14] A.Z. Panagiotoupoulos, R.C. Reid, ACS Symp. Ser. 300 (1986) 571–582.

[15] M.J. Huron, J. Vidal, Fluid Phase Equilib. 3 (1979) 255–271.

[16] D.S. Abrams, J.M. Prausnitz, AIChE J. 21 (1975) 116–128.

[17] D.R. Lide, H.P.R. Frederikse, CRC Handbook of Chemistry and Physics, 80th ed., CRC Press Inc., Boca Raton, FL, 1999.

[18] T.E. Daubert, R.P. Danner, Physical and Thermodynamic Properties of Pure Chemicals: Data Compilation, Hemisphere, New York, 1989.

[19] J.A. Riddick, W.B. Bunger, T.K. Sakano, Organic Solvents: Physical Properties and Methods of Purification, fourth ed., John Wiley & Sons, New York, 1986.